Experimental

Matrix Synthesis: {(BuSn)$_{12}$O$_{14}$(OH)$_6$}(OH)$_2$ was prepared according to previously described methods [13,20]. The two different poly(ethylene glycol) bis(carboxymethyl) ethers, HO$_2$CCH$_2$O(CH$_2$CH$_2$O)$_n$CH$_2$CO$_2$H, were purchased from Aldrich. Their molecular weights were determined by titrating their acidity (in water), according to the presence of two acid functions per polymer. PEG1 ($M_w = 255$ g/mol, $<n> = 2.75$) is a waxy solid and PEG2 ($M_w = 630$ g/mol, $<n> = 11.3$) is a highly viscous liquid. Reactions between {(BuSn)$_{12}$O$_{14}$(OH)$_6$}(OH)$_2$ and carboxymethyl-terminated PEG were carried out as follows: To a 5 wt.-% solution of {(BuSn)$_{12}$O$_{14}$(OH)$_6$}(OH)$_2$ in THF was added drop by drop a 10 wt.-% solution of a carboxymethyl-terminated PEG, or a mixture of both, in THF. The amount of PEG solution added was adjusted to obtain final –CO$_2$H/{(BuSn)$_{12}$O$_{14}$(OH)$_6$}(OH)$_2$ ratios of 2. After adding the carboxymethyl-terminated PEG, the solutions remain clear. The systems were then dried under vacuum to remove the THF and generated water. Samples ranging from powders to waxy solids were obtained.

Materials Processing: SO1 was purchased from Aldrich and SO2 was a gift from James Robinson Ltd. (England). The dried hybrid materials were redissolved in THF along with the dyes. The doped solutions were spin-coated ($\omega = 700$–1000 rpm) onto glass substrates and dried in air.

Characterization: Solid-state MAS ^{119}Sn and ^{13}C NMR experiments were carried out on a Bruker MSL300 spectrometer (111.92 MHz and 75.47 MHz for ^{119}Sn and ^{13}C, respectively). ^{13}C CP MAS NMR spectra were obtained with a contact time of 2 ms and a recycling delay of 5 s. ^{13}C chemical shifts are referenced (0 ppm) versus external tetramethylsilane. ^{119}Sn MAS NMR spectra were obtained using direct polarization. The pulse angle was about 30° (~1 µs), the spectral width was 200 000 Hz and the recycling delay 15 s. ^{119}Sn chemical shifts are referenced to tetramethyltin (0 ppm) using tetracyclohexyltin (–97.35 ppm) as a secondary external reference. At least two different spinning rates were used to assign unambiguously the isotropic ^{119}Sn resonances. To determine the relative proportions of every site, ^{119}Sn MAS NMR spectra were simulated with WinFit [32]. This software was also used to compute the ^{119}Sn shielding tensorial values, using the Herzfeld and Berger approach [33]. They are reported as the isotropic chemical shift ($\delta_{iso} = -\sigma_{iso} = -(\sigma_{11} + \sigma_{22} + \sigma_{33})/3$; σ_{ii} being the tensorial values in the principal axis system), the anisotropy ($\zeta = \sigma_{33} - \sigma_{iso}$), and the asymmetry ($\eta = |\sigma_{11} - \sigma_{22}| / |\sigma_{33} - \sigma_{iso}|$), with the following sorting protocol: $|\sigma_{33} - \sigma_{iso}| > |\sigma_{11} - \sigma_{iso}| \geq |\sigma_{22} - \sigma_{iso}|$ [34,35].

^{119}Sn solution NMR spectra were obtained on a Bruker AC300 spectrometer (111.92 MHz for ^{119}Sn) under proton decoupling. FTIR experiments were run on a Nicolet Magna 550 spectrometer. Samples were mixed with KBr and pressed into pellet. UV-vis spectra were obtained on a Kontron Uvikon 940 spectrometer. Photocoloration was performed with a 400 W Xe lamp equipped with filters to select the irradiation wavelength. DSC experiments were run on a TA Instrument DSC 2010 apparatus with heating rates of 20 °C min^{-1} from –150 to +180 °C. T_g was always measured at the inflexion point of the second run to make sure that the thermal history of the samples was cleared up by the first temperature ramp.

[1] Special issue on Hybrid Organic–Inorganic Materials, *Chem. Mater.* **2001**, *13(10)*.
[2] B. M. Novak, *Adv. Mater.* **1993**, *5*, 422.
[3] *Proc. of the First European Workshop on Hybrid Organic–Inorganic Materials* (Eds: C. Sanchez, F. Ribot), *New J. Chem.* **1994**, *18(10)*.
[4] U. Schubert, N. Hüsing, A. Lorenz, *Chem. Mater.* **1995**, *7*, 2010.
[5] D. A. Loy , K. J. Shea, *Chem. Rev.* **1995**, *95*, 1431.
[6] *Applied Photochromic Polymer Systems* (Ed: C. B. McArdle), Blackie Academic & Professional, London **1992**.
[7] a) D. Levy, D. Avnir, *J. Phys. Chem.* **1988**, *92*, 4734. b) D. Levy, S. Einhorn, D. Avnir, *J. Non-Cryst. Solids* **1989**, *113*, 137.
[8] D. Levy, *Chem. Mater.* **1997**, *9*, 2666.
[9] C. Sanchez, B. Lebeau, *MRS Bull.* **2001**, *26*, 377.
[10] F. Ribot, C. Sanchez, *Comments Inorg. Chem.* **1999**, *20*, 327.
[11] C. Sanchez, G. J. de A. A. Soler-Illia, F. Ribot, T. Lalot, C. R. Mayer, V. Cabuil, *Chem. Mater.* **2001**, *13*, 3061.
[12] G. J. de A. A. Soler-Illia, L. Rozes, M.-K. Boggiano, C. Sanchez, C.-O. Turrin, A.-M. Caminade, J.-P. Majoral, *Angew. Chem. Int. Ed.* **2000**, *39*, 4249.
[13] F. Banse, F. Ribot, P. Tolédano, C. Sanchez, *Inorg. Chem.* **1995**, *34*, 6371.
[14] D. Dakternieks, H. Zhu, E. R. T. Tiekink, R. J. Colton, *J. Organomet. Chem.* **1994**, *476*, 33.
[15] H. Puff, H. Reuter, *J. Organomet. Chem.* **1989**, *373*, 173.

[16] C. Eychenne-Baron, F. Ribot, N. Steunou, C. Sanchez, F. Fayon, M. Biesemans, J. C. Martins, R. Willem, *Organomet.* **2000**, *19*, 1940.
[17] J. Beckmann, K. Jurkschat, U. Kaltenbrunner, S. Rabe, M. Schürmann, D. Dakternieks, A. Duthie, D. Müller, *Organometallics* **2000**, *19*, 4887.
[18] F. Ribot, F. Banse, F. Diter, C. Sanchez, *New J. Chem.* **1995**, *19*, 1163.
[19] F. Ribot, C. Eychenne-Baron, F. Banse, C. Sanchez, *Mater. Res. Soc. Symp. Proc.* **1996**, *435*, 43.
[20] C. Eychenne-Baron, F. Ribot, C. Sanchez, *J. Organomet. Chem.* **1998**, *567*, 137.
[21] F. Ribot, F. Banse, C. Sanchez, M. Lahcini, B. Jousseaume, *J. Sol-Gel Sci. Technol.* **1997**, *8*, 529.
[22] L. Angiolini, D. Caretti, C. Carlini, R. de Vito, F. T. Niesel, E. Salatelli, F. Ribot, C. Sanchez, *J. Inorg. Organomet. Polym.* **1998**, *7*, 151.
[23] F. Ribot, C. Sanchez, R. Willem, J. C. Martins, M. Biesemans, *Inorg. Chem.* **1998**, *37*, 911.
[24] H. Reuter, A. Sebald, *Z. Naturforsh.* **1993**, *48b*, 195.
[25] K. Nakamoto, *Infrared and Raman Spectra of Inorganic and Coordination Compounds*, Wiley, New York, **1978**.
[26] C. Reichardt, *Solvents and Solvent Effects in Organic Chemistry*, Wiley-VCH, Weinheim **1998**.
[27] H. Dürr, H. Bouas-Laurent, *Photochromism: Molecules and Systems*, Elsevier, Amsterdam **1990**.
[28] Y. Atassi, *Ph.D. Thesis*, Ecole Nationale Supérieure de Cachan, France **1996**.
[29] L. Hou, H. Schmidt, *J. Mater. Sci.* **1996**, *31*, 3427.
[30] a) B. Schaudel, C. Guermeur, C. Sanchez, K. Nakatani, J. Delaire, *J. Mater. Chem.* **1997**, *7*, 61. b) G. Winrsberger, B. J. Scott, B. F. Chmelka, G. D. Stucky, *Adv. Mater.* **2000**, *12*, 1450.
[31] For SO1 and SO2 the absorption maximum of the merocyanines opened forms shift towards longer wavelength (bathochromic effect) with increasing solvent polarity. The shift for SO1 is about 18 nm from toluen to ethanol.
[32] D. Massiot, H. Thiele, A. Germanus, *Bruker Rep.* **1994**, *140*, 43.
[33] J. Herzfeld, A. E. Berger, *J. Chem. Phys.* **1980**, *73*, 6021.
[34] U. Haeberlen, *Adv. Magn. Reson. Suppl. 1* **1976**.
[35] R. K. Harris, S. E. Lawrence, S. W. Oh, *J. Mol. Struct.* **1995**, *347*, 309.

Synthesis of Submicrometer-Sized Hollow Silver Spheres in Mixed Polymer–Surfactant Solutions**

By *Dongbai Zhang, Limin Qi,* *Jiming Ma,*
and *Humin Cheng*

Inorganic hollow spheres of nanometer to micrometer dimensions represent an important class of materials that have wide potential applications, such as controlled release capsules of various substances (e.g., drugs, cosmetics, dyes, and inks), artificial cells, catalysts, fillers, coatings, pigments, and light-weight structural materials, owing to their low density, large specific area, mechanical and thermal stability, and surface permeability.[1–4] Recent efforts to prepare inorganic hollow spheres have been focused on inorganic precipitation processes against a variety of sacrificial templates, including polystyrene latex spheres[5–7] and their crystalline arrays,[2] resin spheres,[3] vesicles,[8,9] liquid droplets,[4,10–13] miniemulsions,[14] microemulsions,[15] polymer micelles,[16] and polymer–surfactant complex micelles.[17] Such templating approaches have been implemented successfully in the synthesis

[*] Prof. L. Qi, D. Zhang, Prof. J. Ma, H. Cheng
College of Chemistry, Peking University
Beijing 100871 (China)
E-mail: liminqi@chem.pku.edu.cn

of inorganic hollow spheres comprising glass, ceramics, semiconductors, magnetic materials, and biominerals. However, there has been only little progress in the templated synthesis of hollow metal spheres, although hollow spheres composed of silica-encapsulated gold nanoparticles have been reported.[18] Actually, metal-coated colloidal core–shell particles have attracted intense interest because of their potential use (both solid and, after core removal, hollow) as catalysts, sensors, substrates in surface-enhanced Raman scattering (SERS), and colloidal entities with unique optical properties.[18,19] In particular, silver-coated latex or silica spheres have been synthesized using a range of wet-chemistry methods.[20–23] However, hollow silver spheres have not been fabricated from core–shell spheres possibly due to the difficulties in retaining the shell structures during core removal.

Double-hydrophilic block copolymers (DHBCs)[24] have been used as a new class of additives for biomimetic synthesis of a variety of inorganic minerals with unusual morphologies[25–27] as well as silver nanowires.[28] Recently, we reported a novel synthesis of micrometer-sized hollow calcite spheres in the presence of DHBC–surfactant complex micelles acting as removable templates.[17] It is expected that this templating process can be extended to the synthesis of hollow metal spheres. In this communication, we report on a one-step facile synthesis of submicrometer-sized hollow silver spheres in the same mixed DHBC–surfactant system, i.e., the mixed poly-(ethylene oxide)-*block*-poly(methacrylic acid)–sodium dodecylsulfate (PEO-*b*-PMAA–SDS) system.[17]

Typically, hollow silver spheres were synthesized by chemical reduction of $AgNO_3$ by ascorbic acid in aqueous solutions of PEO-*b*-PMAA (1 g L^{-1}) and SDS (10 mM). Figure 1 presents a typical X-ray diffraction (XRD) pattern of the obtained hollow silver spheres; sharp diffraction peaks corre-
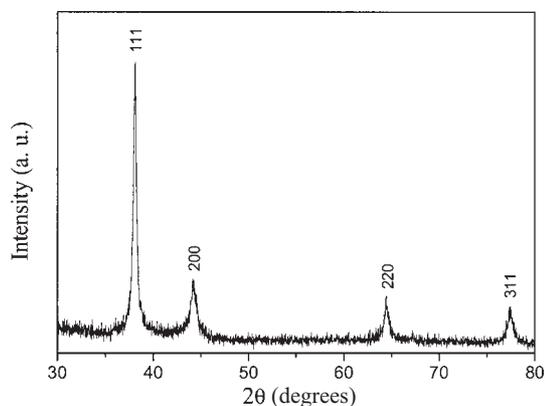

Fig. 1. XRD pattern of hollow silver spheres formed in mixed PEO-*b*-PMAA–SDS solution. [SDS] = 10 mM.

sponding to the cubic structure of metallic Ag are observed, indicating the formation of pure silver of high crystallinity. The typical scanning electron microscopy (SEM) image shown in Figure 2a suggests that the product consists of well-defined hollow silver spheres ranging in size from 260 nm to 1.2 μm with an average diameter of ca. 630 nm. Broken hol-
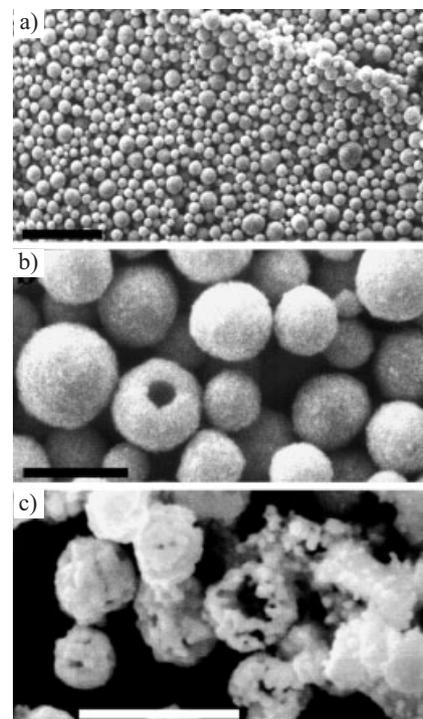

Fig. 2. SEM images of hollow silver spheres formed in mixed PEO-*b*-PMAA–SDS solution before (a,b) and after (c) sonication. [SDS] = 10 mM. Scale bars: a) 5 μm, b) 1 μm, c) 1 μm.

low spheres are occasionally observed. Although, from SEM observation the proportion of broken spheres appears to be less than 1 %, the actual proportion could be somewhat larger as there may be some broken spheres with their holes upside down. A partly broken hollow sphere can be clearly seen in the high-magnification SEM image in Figure 2b, which also indicates that the outer surface of these spheres is not perfectly smooth. It was found that the hollow spheres could be broken by extensive sonication. As shown in Figure 2c, the hollow spheres were broken to different extents after 15 min of sonication. Most spheres exhibited coarser surfaces with a few small holes on the surfaces whereas a very small proportion of the spheres were broken to a large extent. Note that the present hollow silver spheres are much more difficult to break compared with the hollow calcite spheres produced previously in a similar templated synthesis,[17] indicating that the silver shells are much more robust than the calcite shells.

To further confirm the hollow nature of the intact spheres, transmission electron microscopy (TEM) images were taken. Figure 3a shows a typical TEM image of intact spheres; they have pale regions in the central parts in contrast to dark edges. This excludes the possibility of solid spheres. However, it is hard to clearly see the hollow interior and to estimate the shell thickness, possibly due to a relatively thick and dense shell consisting of metallic silver. Therefore, we tried to partly dissolve the silver spheres in 3 M HNO_3 solution to reveal their hollow structures. After treatment with 3 M HNO_3 for 10 min, partly dissolved spheres remained, clearly showing their shell structure with shell thickness ranging from 50 to
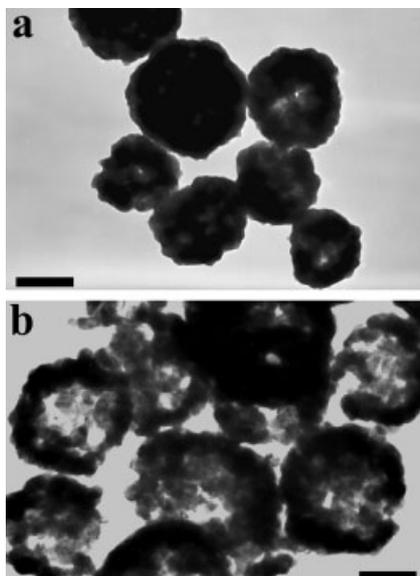
Fig. 3. TEM images of hollow silver spheres formed in mixed PEO-*b*-PMAA–SDS solution before (a) and after (b) treatment with HNO$_3$. [SDS] = 10 mM. Scale bars: 200 nm.

Fig. 4. TEM (a) and SEM (b,c) images of silver samples obtained in mixed PEO-*b*-PMAA–SDS solutions: a) [SDS] = 0 mM, b) [SDS] = 5 mM, c) [SDS] = 20 mM. Scale bars: a) 200 nm, b) 1 μm, c) 5 μm.

100 nm (Fig. 3b). The corresponding density measurement revealed that the hollow spheres have a density of 6.0 g cm^{-3}. Thermogravimetric analysis (TGA) revealed that there is essentially no weight loss up to 800 °C, indicating that the silver shells, consisting of primary silver particles, are not completely solid and the polymer and surfactant can be washed out through small holes inside the closed shells. Accordingly, an average shell thickness of about 80 nm, a value in good agreement with the observed thickness, was estimated based on the known density of silver (10.5 g cm^{-3}) and the average sphere diameter (~630 nm). Therefore, we have demonstrated that submicrometer-sized hollow silver spheres can be readily synthesized in the mixed PEO-*b*-PMAA–SDS system. To the best of our knowledge, this is the first solution synthesis of hollow spheres of noble metals.

As the SDS concentration was found to have a significant influence on the formation of hollow calcite spheres in the mixed PEO-*b*-PMAA–SDS system, we studied the effect of the SDS concentration on the formation of hollow silver spheres in a similar way. If the polymer concentration was kept at 1 g L^{-1} and no SDS was present in the solution, curved or distorted silver nanowires ranging in diameter from 40 to 80 nm were produced (Fig. 4a), reminiscent of the silver nanowires (20–40 nm in diameter) obtained in PEO-*b*-PMAA solutions without the presence of additional reductants.[28] This indicates that the presence of the reductant ascorbic acid results in the formation of silver nanowires with larger diameters. If 5 mM SDS was present in the solution, silver particles about 400 nm in diameter, with rather coarse surfaces, and looking like entangled nanowires were produced (Fig. 4b). The corresponding density measurement gave a value nearly identical to 10.5 g cm^{-3}, indicating that the obtained particles are solid rather than hollow. It seems that these solid silver particles represent a transition state between the silver nano-
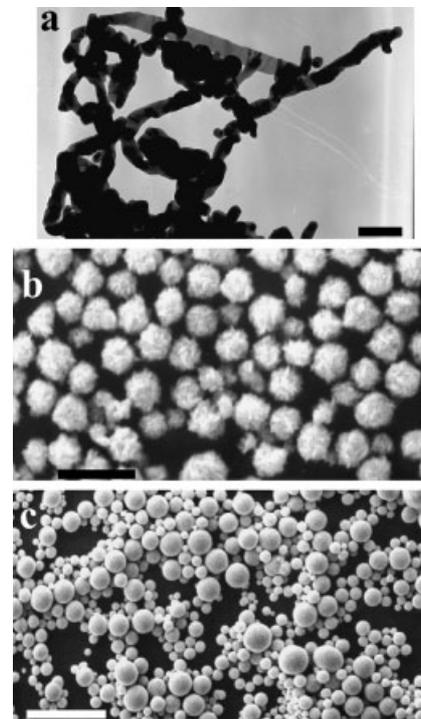
wires (Fig. 4a) and the hollow silver spheres obtained at a SDS concentration of 10 mM (Fig. 2a). When the SDS concentration in the mixed PEO-*b*-PMAA–SDS solution was further increased to 20 mM, the product was hollow silver spheres with smoother surfaces and a lower density (~3.8 g cm^{-3}). These spheres were considerably more polydisperse with sizes ranging from 270 nm to 2 μm.

It is proposed that the formation mechanism of the present hollow silver spheres is essentially the same as that proposed for the formation of hollow calcite spheres in the mixed PEO-*b*-PMAA–SDS system.[17] This means that core–shell micelles are formed by the PEO-*b*-PMAA–SDS complex with a core of PEO segments solubilized in the head group region of the SDS micelles, and a shell of PMAA segments. Such core–shell micelles with a PMAA corona would act as templates for the precipitation of silver due to the strong coordination interaction between the anionic PMAA block and Ag$^+$ ions. Preliminary dynamic light scattering studies have revealed that the size of the PEO-*b*-PMAA–SDS complex micelles in the absence of foreign ions is about 100–200 nm.[17] Assuming a shell thickness of 80 nm, the inner diameter of the smallest hollow silver spheres (260 nm) would be about 100 nm, which is of the same length scale as that of the aggregate templates. For larger hollow spheres, their inner diameters could be much larger than the aggregate size; however, the proposed mechanism is still reasonable considering that both the presence of the reactants in the solution and the development of the inorganic structure could perturb the organic template, resulting in an adaptive construction.[17] It is noteworthy that

the present hollow silver spheres are much smaller than the previous hollow calcite spheres (ca. 3.4 μm), which could be attributed to the stronger coordination interaction of the anionic PMAA block with Ag^+ ions than with Ca^{2+} ions. This stronger coordination interaction could also be a large contributory factor to the considerable increase of the minimum SDS concentration required for the formation of hollow spheres, i.e., from 1 mM SDS for hollow calcite spheres to 10 mM SDS for hollow silver spheres. In other words, the presence of free PEO-*b*-PMAA molecules in the solution at a lower SDS concentration would be helpful for calcite precipitation around the complex micelles as the polymer acts as an inhibitor,[17] but would induce separate silver precipitation away from the complex micelles due to the formation of PEO-*b*-PMAA–Ag^+ complex.[28]

In conclusion, submicrometer-sized hollow silver spheres were successfully synthesized by using PEO-*b*-PMAA–SDS complex micelles as templates. The unique silver shell structures obtained here may be promising candidates for both fundamental research and applications. It is believed that templated synthesis based on polymer–surfactant complex micelles represents a novel route to inorganic hollow spheres, which is a topic of intense interest.

Experimental

A commercial DHBC, poly(ethylene oxide)-*block*-poly (methacrylic acid) (PEO-*b*-PMAA, PEO = 3000 g/mol, PMAA = 700 g/mol, T. Goldschmidt AG) [26], was used in this work. The anionic PMAA block carries carboxylate groups capable of coordinating with Ag^+ ions, whereas the non-ionic PEO block mainly promotes solubilization in water [28]. The reduction of $AgNO_3$ by ascorbic acid was conducted at room temperature (ca. 22 °C) in aqueous solutions of PEO-*b*-PMAA and the anionic surfactant sodium dodecyl sulfate (SDS) [17]. Briefly, 9 mL of solution containing PEO-*b*-PMAA (10 mg), SDS (typically, 0.1 mmol), and ascorbic acid (0.2 mmol) was prepared first. Then, 1 mL of 0.2 M $AgNO_3$ was added under vigorous stirring, which gave a final PEO-*b*-PMAA concentration of 1 g L^{-1} and final reactant ($AgNO_3$ and ascorbic acid) concentrations of 0.02 M. After 1 min of stirring, the solution was allowed to stand for 24 h, followed by centrifugation and washing with water repeatedly. The collected products were characterized with scanning electron microscopy (SEM), transmission electron microscopy (TEM), X-ray diffraction (XRD), thermogravimetric analysis (TGA), and density measurements.

[1] F. Caruso, *Chem. Eur. J.* **2000**, *6*, 413.
[2] Z. Zhong, Y. Yin, B. Gates, Y. Xia, *Adv. Mater.* **2000**, *12*, 206.
[3] A. B. Bourlinos, M. A. Karakassides, D. Petridis, *Chem. Commun.* **2001**, 1518.
[4] C. E. Fowler, D. Khushalani, S. Mann, *J. Mater. Chem.* **2001**, *11*, 1968.
[5] K. H. Rhodes, S. A. Davis, F. Caruso, B. Zhang, S. Mann, *Chem. Mater.* **2000**, *12*, 2832.
[6] R. A. Caruso, A. Susha, F. Caruso, *Chem. Mater.* **2001**, *13*, 400.
[7] F. Caruso, X. Shi, R. A. Caruso, A. Susha, *Adv. Mater.* **2001**, *13*, 740.
[8] D. H. W. Hubert, M. Jung, P. M. Frederik, P. H. H. Bomans, J. Meuldijk, A. L. German, *Adv. Mater.* **2000**, *12*, 1286.
[9] H. T. Schmidt, A. E. Ostafin, *Adv. Mater.* **2002**, *14*, 532.
[10] C. E. Fowler, D. D. Khushalani, S. Mann, *Chem. Commun.* **2001**, 2028.
[11] J. Huang, Y. Xie, B. Li, Y. Liu, Y. Qian, S. Zhang, *Adv. Mater.* **2000**, *12*, 808.
[12] X. Gao, J. Zhang, L. Zhang, *Adv. Mater.* **2002**, *14*, 290.
[13] P. Tartaj, T. Gonzalez-Carreno, C. J. Serna, *Adv. Mater.* **2001**, *13*, 1620.
[14] B. Putlitz, K. Landfester, H. Fischer, M. Antonietti, *Adv. Mater.* **2001**, *13*, 500.
[15] D. Walsh, B. Lebeau, S. Mann, *Adv. Mater.* **1999**, *11*, 324.
[16] T. Liu, Y. Xie, B. Chu, *Langmuir* **2000**, *16*, 9015.
[17] L. Qi, J. Li, J. Ma, *Adv. Mater.* **2002**, *14*, 300.
[18] F. Caruso, M. Spasova, V. Salgueirino-Maceria, L. M. Liz-Marzan, *Adv. Mater.* **2001**, *13*, 1090.
[19] D. I. Gittins, A. S. Susha, B. Schoeler, F. Caruso, *Adv. Mater.* **2002**, *14*, 508.
[20] A. B. R. Mayer, W. Grebner, R. Wannemacher, *J. Phys. Chem. B* **2000**, *104*, 7278.
[21] A. G. Dong, Y. J. Wang, Y. Tang, N. Ren, W. L. Yang, Z. Gao, *Chem. Commun.* **2002**, 350.
[22] Y. Kobayashi, V. Salgueirino-Maceira, L. M. Liz-Marzan, *Chem. Mater.* **2001**, *13*, 1630.
[23] V. G. Pol, D. N. Srivastava, O. Palchik, M. A. Slifkin, A. M. Weiss, A. Gedanken, *Langmuir* **2002**, *18*, 3352.
[24] A recent review: H. Cölfen, *Macromol. Rapid Commun.* **2001**, *22*, 219.
[25] L. Qi, H. Cölfen, M. Antonietti, *Angew. Chem. Int. Ed.* **2000**, *39*, 604.
[26] H. Cölfen, L. Qi, *Chem. Eur. J.* **2001**, *7*, 106.
[27] M. Antonietti, M. Breulmann, C. G. Göltner, H. Cölfen, K. K. Wong, D. Walsh, S. Mann, *Chem. Eur. J.* **1998**, *4*, 2493.
[28] D. Zhang, L. Qi, J. Ma, H. Cheng, *Chem. Mater.* **2001**, *13*, 2753.

Fabrication of Diffractive and Micro-optical Elements Using Microlens Projection Lithography**

By *Ming-Hsien Wu* and *George M. Whitesides**

Arrays of optical microstructures—gratings, beam splitters, lenses, mirrors—are useful in many types of devices such as optical processing systems,[1–3] and microelectromechanical systems (MEMS).[4,5] The quality of these elements depends on their surface profiles and uniformity. Arrays of optical elements have been produced by many methods, including conventional photolithography,[6] laser pattern writing,[7] photography,[8,9] plastic molding,[10] interference lithography,[11] ion-beam lithography,[12,13] X-ray lithography,[14] and conventional gray-scale lithography.[15–17] Although these methods produce uniform elements with controlled surface profiles, they require the use of expensive facilities (e.g., mask aligners or laser optical systems) or templates (e.g. master molds or gray-scale photomasks with sub-micrometer resolution). Some of these techniques (e.g., laser pattern writing and photography) produce microelements with limited resolution (> 1 μm); they cannot, as a result, control the surface relief of the elements at sub-micrometer resolution. Techniques such as interference lithography produce microstructures with sizes, periods, and arrangements limited by the incident wavelengths and angles. All these techniques are relatively expensive and inconvenient.

In this paper, we demonstrate a simple, low-cost method for the fabrication of both diffractive optical elements and arrays of micro-optical elements using microlens arrays for projec-

[*] Prof. G. M. Whitesides, Dr. M.-H. Wu
Department of Chemistry and Chemical Biology, Harvard University
12 Oxford Street, Cambridge, MA 02138 (USA)
E-mail: gwhitesides@gmwgroup.harvard.edu